Biogeosciences
Discussions

EGU

Open Access

Overcalcified forms of the coccolithophore *Emiliania huxleyi* in high CO$_2$ waters are not pre-adapted to ocean acidification.

Peter von Dassow[1,2,3*], Francisco Díaz-Rosas[1,2], El Mahdi Bendif[4], Juan-Diego Gaitán-Espitia[5], Daniella Mella-Flores[1], Sebastian Rokitta[6], Uwe John[6], and Rodrigo Torres[7,8]

[1] Facultad de Ciencias Biológicas, Pontificia Universidad Católica de Chile, Santiago, Chile.
[2] Instituto Milenio de Oceanografía de Chile.
[3] UMI 3614, Evolutionary Biology and Ecology of Algae, CNRS-UPMC Sorbonne Universités, PUCCh, UACH.
[4] Department of Plant Sciences, University of Oxford, OX1 3RB Oxford, UK.
[5] CSIRO Oceans and Atmosphere, GPO Box 1538, Hobart 7001, TAS, Australia.
[6] Marine Biogeosciences | PhytoChange Alfred Wegener Institute – Helmholtz Centre for Polar and Marine Research, Bremerhaven, Germany.
[7] Centro de Investigación en Ecosistemas de la Patagonia (CIEP), Coyhaique, Chile.
[8] Centro de Investigación: Dinámica de Ecosistemas marinos de Altas Latitudes (IDEAL), Punta Arenas, Chile.

Correspondence to: Peter von Dassow (pvondassow@bio.puc.cl)

Abstract. Marine multicellular organisms inhabiting waters with natural high fluctuations in pH appear more tolerant to acidification than conspecifics occurring in nearby stable waters, suggesting that environments of fluctuating pH hold genetic reservoirs for adaptation of key groups to ocean acidification (OA). The abundant and cosmopolitan calcifying phytoplankton *Emiliania huxleyi* exhibits a range of morphotypes with varying degrees of coccolith mineralization. We show that *E. huxleyi* populations in the naturally acidified upwelling waters of the Eastern South Pacific, where pH drops below 7.8 as is predicted for the global surface ocean by the year 2100, are dominated by exceptionally overcalcified morphotypes whose distal coccolith shield can be almost solid calcite. Shifts in morphotype composition of *E. huxleyi* populations correlate with changes in carbonate system parameters. We tested if these correlations indicate that the hypercalcified morphotype is adapted to OA. In experimental exposures to present-day vs. future pCO$_2$ (400 µatm vs. 1200 µatm), the overcalcified morphotypes showed the same growth inhibition (-29.1±6.3%) as moderately calcified morphotypes isolated from non-acidified water (-30.7±8.8%). Under OA conditions, production rates of particulate organic carbon (POC) increased, while production rates of particulate inorganic carbon (PIC) were maintained or decreased slightly (but not significantly), leading to lowered PIC/POC ratios in all strains. There were no consistent correlations of response intensity with strain origin. OA affected coccolith morphology equally or more strongly in overcalcified strains compared to moderately calcified strains. OA conditions appear not to directly select for exceptionally overcalcified morphotypes over other morphotypes directly, but perhaps indirectly by ecologically correlated factors. More generally, these results suggest that oceanic planktonic microorganisms, despite their rapid turn-over and large population sizes, do not necessarily exhibit adaptations to naturally high CO$_2$ upwellings, and this ubiquitous coccolithophore may be near a limit of its capacity to adapt to ongoing ocean acidification.

1 Introduction

Coccolithophores are planktonic single-celled photoautotrophs mostly in the range 3-20 µm and characterized by bearing calcite plates (coccoliths) (Tyrrell and Young, 2009) and represent one of the most abundant and widespread groups of marine eukaryotic phytoplankton (Iglesias-Rodríguez et al., 2002; Litchman et al., 2015). In addition to being important primary producers, coccolithophores contribute most of the calcium carbonate (CaCO$_3$) precipitation in pelagic systems. Although CaCO$_3$ precipitation in the surface is a source of CO$_2$, i.e., the 'carbonate counter pump' (Frankignoulle et al., 1994), CaCO$_3$ may enhance sinking of organic matter by imposing a ballast effect on sinking aggregates (Armstrong et al., 2002; Sanders et al., 2010) and its dissolution at depth may consume more CO$_2$ than is released at the surface (Smith, 2013). Thus, this plankton functional group has a complex role in ocean carbon cycles. Roughly a third of current anthropogenic

CO$_2$ emissions are being absorbed in the ocean (Sabine et al., 2004), driving a decrease in pH, the conversion of CO$_3^{2-}$ to HCO$_3^-$, and a drop in saturation states of the CaCO$_3$ minerals aragonite and calcite ($\Omega_{aragonite}$, $\Omega_{calcite}$), phenomena collectively termed ocean acidification (OA; Orr et al., 2005). Although most surface waters are expected to remain super-saturated with respect to calcite ($\Omega_{calcite}$ >1), which is less soluble than aragonite, the drop in $\Omega_{calcite}$ might still result in decreases in calcite

5   biomineralization (Hofmann and Schellnhuber, 2009). Understanding the response of coccolithophores to OA is thus needed for predicting how pelagic ecosystems and the relative intensity of the biological carbon pumps will change as atmospheric CO$_2$ continues to increase.

Many studies designed to assess coccolithophores´ responses to OA have been performed in short-term culture and mesocosm experiments on time-scales of weeks to months, and carbonate systems were usually manipulated to mimic pre-

10   industrial, present and future CO$_2$ levels. Mesocosm studies have shown that North Sea populations of the cosmopolitan and abundant species *Emiliania huxleyi* are negatively impacted by OA (Engel et al., 2005; Riebesell et al., 2017). However, a wide range of OA responses of growth, calcification (PIC) and productivity (POC) have been reported in laboratory cultures of *E. huxleyi*, mostly using different regional strains (Riebesell et al., 2000; Iglesias-Rodriguez et al., 2008; Langer et al., 2009; Müller et al., 2015, 2017; Brady Olson et al., 2017; Jin et al., 2017). According to a recent comprehensive review and

15   meta-analysis (Meyer and Riebesell, 2015), the mean responses of *E. huxleyi* averaged over 19 studies indicated that OA has a negative effect on PIC quotas and production rates as well as PIC/POC ratios, but no consistent effects on POC quotas and production rates. The response variability among strains of *E. huxleyi* (Langer et al., 2009; Müller et al., 2015) is also seen within the genus *Calcidiscus* (Diner et al., 2015), and suggests a high potential for genetic adaptation within coccolithophores.

20   Such adaptive capacity to OA has been suggested for *E. huxleyi* in lab-based long-term experimental evolution studies (up to 2000 generations) on clonal strains (Lohbeck et al., 2012; Schlüter et al., 2016). It is still difficult to know to which extent such experiments reflect real-world adaptation processes. First, only asexually propagating cells have yet been explored in the lab, while sexual recombination in natural populations is expected to accelerate adaptation (McDonald et al., 2016). Second, calcification is costly and in nature must be maintained by providing benefits to the cell. The ecological purpose,

25   however, remains unclear, and it has been suggested that the coccosphere may serve for defence against grazing or parasites, for modifying light/UV levels reaching the cell, or even other purposes (Monteiro et al., 2016). The long-term and non-linear declines in calcification observed in experimental adaptation to high pCO$_2$ (Schlüter et al., 2016) thus might have a high potential cost if such changes occurred in nature.

Complementary to experimental approaches, observational studies that correlate coccolithophore communities and levels or

30   rates of calcification with variability in carbonate system parameters offer important insights into possible adaptations to OA. Focusing only on *E. huxleyi* and the closely related genus *Gephyrocapsa* (both within the family Noëlaerhabdaceae), a general pattern has been documented of a decreasing levels of calcification with increasing pCO$_2$ was observed in both, modern and recent fossil coccolithophores across the world´s ocean basins (Beaufort et al., 2011). This pattern involved shifts away from more heavily calcified *Gephyrocapsa* that dominated assemblages under the lowest pCO$_2$, towards a

35   spectrum of *E. huxleyi* morphotypes that were more abundant under intermediate and high pCO$_2$: *E. huxleyi* 'type A' morphotypes with heavier coccoliths (more calcite per coccolith) dominated *E. huxleyi* populations in waters with intermediate pCO$_2$ while 'type B/C' or 'type C' morphotypes with successively lighter coccoliths, dominated in higher pCO$_2$ waters (Beaufort et al., 2011; Poulton et al., 2011).

Beyond this comparably clear pattern, the survey by Beaufort et al. (2011) also reported one important exception to the

40   general trend: At two sites approaching the Chilean upwelling zone, forms of *E. huxleyi* with exceptionally over-calcified coccoliths dominated in naturally acidified upwelling waters, where pCO$_2$ reaches values more than two-fold higher than the equilibrium with present-day atmosphereic levels. Similarly, a year-long monthly survey of coccolithophore communities in the Bay of Biscay found that an over-calcified type A form dominated during the winter, when pCO$_2$ was highest, but

contributed only a minor part to the *E. huxleyi* populations in summer, when pCO_2 was lowest (Smith et al., 2012). One explanation might be that over-calcified morphotypes are especially tolerant to such OA conditions.

The Eastern South Pacific in front of Chile and Peru presents a natural laboratory for investigating such hypotheses regarding organisms´ responses to ocean acidification. The coastal zone is naturally acidified, with surface waters frequently

5   reaching pCO_2 levels >1000 µatm and pH values < 7.7 during upwelling events (Friederich et al., 2008; Torres et al., 2011). In this study, we surveyed the coccolithophore communities of the Chilean upwelling zone as well as adjacent coastal and offshore waters with varying pCO_2 levels and isolated *E. huxleyi* strains of dominant morphotypes. In lab-based experiments, three strains showing distinct over-calcification were compared with two moderately calcified type-A morphotypes in terms of their response to OA (400 vs. 1200 µatm pCO_2) to investigate whether CO_2 might indeed be the environmental driver

10 selecting for the extreme overcalcified morphotypes specific to the Chilean coast.

2 Materials and Methods

2.1 Surveys

An oceanographic cruise (NBP 1305) was conducted on board R/V *Nathaniel B. Palmer* (NBP) during the early austral winter (27 June-22 July 2013) along a transitional zone from coastal to open ocean waters off central-south Peru and north

15 Chile (Fig. 1A). A total of 24 stations were sampled between 22°S and 13° S and from 70° W to 86° W (ranging from 47 to 1424 km from the coast). Central Chile coastal surveys were conducted on board the R/V Stella Maris II (Universidad Católica de Norte) during the mid-spring of 2011 (12 October) and 2012 (28 November) and aboard a rented fishing launch (18-19 November 2012) in the high pCO_2 upwelling zone in front of Tongoy Bay (TON), north Chile (~30°S-72°W; Fig. 1B). These two coastal surveys consisted of 7 sampling points distributed between 1 and 23 km off the coast. Another

20 coastal sampling was conducted from a small launch (belonging to the Pontificia Universidad Católica de Chile) during the mid-spring of 2012 (10 November), in the upwelling zone in front of El Quisco Bay (QUI ~33°S-72°W; Fig. 1B). This coastal survey consisted of 1 sampling point located at 4 km offshore. Finally, one sampling was conducted from a rented fishing vessel during the mid-spring of 2011 (01 November), in the mesotrophic waters (MES) that surround the Juan Fernández Islands (JF; ~33°S-78°W; Fig. 1B).

25 ### 2.2 Physical-chemical oceanographic parameters

During the NBP cruise, temperature and salinity were measured with a SBE 25 CTD (Sea-Bird Scientific, Bellevue, WA, USA) from rosette casts or from the on-board running seawater system equipped with a SBE 45 conductivity sensor and a SBE 38 temperature sensor (both from Sea-Bird Scientific). During the 2011 cruise on the R/V Stella Maris II, an SBE 19 *plus* CTD was used (data courtesy of B. Yannicelli). In other samplings, an SBE 18 plus CTD was used for water column

30 measurements. In the 29 November 2012 cruise on the R/V Stella Maris II, surface samples were pumped continuously onboard in underway sampling and analysed with a YSI Pro30 salinometer/thermometer (YSI, Yellow Springs, OH, USA). In October 2011 and November 2012, duplicate 500 mL of surface seawater were collect into borosilicate bottles, fixed with 50µL of $HgCl_2$ saturated solution and stored until measurements for Total Carbon (CT) and Total Alkalinity (AT). Total Alkalinity (AT) was determined by potentiometric titration in an open cell (Heraldsson et al., 1997). The accuracy was

35 controlled against a certified reference material (CRM Bath 115 bottled on September 2011) supplied by Andrew Dickson (Scripps Institution of Oceanography, http://andrew.ucsd.edu/co2qc/batches.html). The correction factor was approximately 1.002. Total carbon (CT), a.k.a. dissolved inorganic carbon (DIC), was determined using a fully automatic dissolved inorganic carbon analyzer (model AS-C3, Apollo SciTech, Newark, DE, USA). All the dissolved carbonate species from a seawater sample were extracted as CO_2 gas by acidification and nitrogen stripping. The CO_2 gas was then quantitatively

40 detected with an infra-red LI-7000 CO_2 Analyzer (LI-COR Environmental, Lincoln, Nebraska USA). Standardization was performed with certified reference material (CRM; Bath 115 bottled on September 2011) supplied by Andrew Dickson

(Scripps Institution of Oceanography). During the expedition off Juan Fernandez (Nov 2011) pH and AT were measured in fixed samples. pH was measured in Total Ion scale using spectrophotometric detection of m-cresol purple absorption in a 100 mm quartz cell thermally regulated at 25.0°C (Dickson et al., 2007). During the NBP cruise, direct measurements of sea surface pCO_2 using NDIR detection were obtained from the ship continuous underway data acquisition system (RVDAS;

5   courtesy of Lamont-Doherty Earth Observatory of Columbia University) in addition to AT samples.

Omega aragonite (Ω_{Ar}) and omega calcite (Ω_{Ca}) and other carbonate system parameters were estimated from the CT-AT pairs (for samplings off the central Chile coast in October 2011 and November 2012), pH-AT (for expedition off Juan Fernandez in November 2011), pCO_2-AT pairs (for NBP 1305 cruise during June-July 2013) using CO2SYS software (Pierrot et al., 2006) set with Mehrbach solubility constants (Mehrbach et al., 1973) refitted by Dickson and Millero

10   (Dickson and Millero, 1987). Environmental parameters are provided in Table S1.

Mean sea surface temperature and chlorophyll a (Chl a) monthly climatologies (2002-2014) were obtained from the Modis Aqua satellite (Feldman, G. C., C. R. McClain, Ocean Color Web, MODIS Aqua Reprocessing R2014.0, NASA Goddard Space Flight Center. Eds. Kuring, N., Bailey, S. W. 23 Dec. 2015. http://oceancolor.gsfc.nasa.gov/) and plotted using SeaDAS (Baith et al., 2001) version 7.1 for mac OSX.

15   **2.3 Phytoplankton analyses**

Discrete seawater samples (Niskin bottles) containing planktonic assemblages were collected at various depths within the upper 150 m, depending on depth of the maximum Chl *a* fluorescence (as proxy of phytoplankton) and from the on-board seawater system when Niskin samples were not available. Duplicate 100 mL samples of seawater (previously filtered through 200 um Nitex mesh) were fixed (final concentration 1% formaldehyde, 0.05% glutaraldehyde, 10 mM borate pH

20   8.5) and stored at 4ºC until light microscopic examination.

Samples were sedimented in 100 mL Utermöhl chambers for 48 h prior to counting. The absolute abundance of microplankton (20-200 μm in size) and coccolithophores (ranging from 2.5-20 μm in size, but mostly comprised of species within the range 3-10 μm including *E. huxleyi*, several species of the genera *Gephyrocapsa*, and *Calcidiscus leptoporus*) were estimated with an inverted microscope (Olympus CKX41) connected to digital camera (Motic 5.0). For counts of large

25   diatoms, thecate dinoflagellates and others planktonic cells (>50 μm in size), a 20x objective was used. For counts of small diatoms and athecate dinoflagellates (<50 μm in size) a 40x objective was used. For counts of total coccolithophores, a 40x objective was used with cross polarized light (Edmund Optics polarizers 54926 and 53347).

In parallel, duplicate 250 mL samples of seawater were filtered onto polycarbonate filters (0.2 μm pore-size; Millipore), which were dried and stored in Petri dishes until processing for identification of coccolithophore species and *E. huxleyi*

30   morphotypes. A small cut portion of each dried filter was sputter-coated with gold. The identification and relative abundance of coccolithophore species was performed by counting a minimum of 80 coccospheres per sample by scanning electron microscopy using either a TM3000 (Hitachi High-Technologies, Tokyo, Japan) or a Quanta 250 (FEI, Hillsboro, Oregon, USA). Classification followed Young et al. (2003). To estimate the absolute abundances of each species within the Nöelaerhabdaceae family, which are difficult to distinguish by light microscopy, the relative abundance of each

35   Nöelaerhabdaceae species determined by SEM counts was multiplied by the absolute abundance of total Nöelaerhabdaceae cells determined from light microscopy counts. SEM images were also used to measure the min. and max. coccosphere diameters and coccolith lengths of each Nöelaerhabdaceae species (ImageJ software version 1.48 for Mac OSX). Also, *E. huxleyi* cells were categorized according to Young et al. (2003), based on the distal shield and central plate of coccoliths. For analysis, they were grouped further: Lightly calcified coccoliths exhibited delicate distal shield elements that are well

40   separated from each other extending from the central area to the outer rim, the central element was completely open, and central area elements were either lacking, lath-like, or plate-like (Fig. 2). These corresponded to the morphotypes B, B/C, C and O (Young et al., 2003; Hagino et al., 2011), a grouping that is supported by recent genetic evidence (Krueger-Hadfield et

4

al., 2014). Moderately calcified coccoliths, corresponding to morphotype A (Young et al., 2003; Hagino et al., 2011), showed thicker distal shield elements that were fused near the central area and often at the rim but were otherwise separated, and a grill central area within a cleanly delimited tube. Two over-calcified morphotypes were observed. One corresponded to the morphotype A-overcalcified type reported in the Bay of Biscay (Smith et al., 2012) with coccolith central areas

5   completely covered or nearly completely covered by elements of the central tube, but distal shield elements not fused (here referred to as A_CC). The second, which we refer to as R/overcalcified, corresponded to R morphotype (distal shield elements fused/slits closed), which exhibited a continuous variation from wide and open central area (Young et al., 2003) to the extreme forms, so far reported only in the Eastern South Pacific (Beaufort et al., 2011), where tube elements had completely or partially overgrown the central area.

10   **2.4 Isolation of *E. huxleyi* strains**

Clonal isolates of coccolithophores were obtained from some stations by isolation of calcified cells using an InFlux Mariner cell sorter as described previously (Von Dassow et al., 2012; Bendif et al., 2016). During the NBP cruise, the InFlux Mariner was in a portable on-board laboratory and isolation of coccolithophores occurred within six hours of sample collection. For other samplings, live seawater samples were hand-carried to Concepción in a cooler with chilled water, and calcified cells

15   were isolated within 24h (without exposure to light or nutrient addition, to minimize possible clonal reproduction between sampling and cell isolation). Calcified strains were identified by SEM and maintained at 15° C (Bendif et al., 2016).

2.5 Experimental testing of *E. huxleyi* responses to high CO_2/low pH

The experiment was performed at the ocean acidification test facility of the Calfuco Marine Laboratory of the Universidad Austral de Chile (Torres et al., 2013). The aim was to investigate the effects of short term exposure to OA

20   conditions similar to those occurring in an upwelling event. The focus was on determining whether there were differences between the heavy calcified morphotypes and moderately calcified morphotypes in response to short-term exposure to CO_2, as would be expected to be experienced by phytoplankton cells from surrounding surface waters inoculating recently upwelled water, where both mooring-mounted and drifter-mounted sensors show pulses of high CO_2 over periods of about a week (Friederich et al., 2008). The OA condition (1200 µatm CO_2) was chosen to represent recently upwelled water based

25   on Torres et al. (1999) compared to CO_2 levels in non-upwelling surface waters (400 µatm). The high CO_2 level of 1200 µatm was also chosen considering previous laboratory studies of the response of *E. huxleyi*: Results of acclimated growth rate in response to short-term changes in the carbonate system manipulated by bubbling have been reported in several studies for two R morphotype strains isolated from the Tasman Sea (where high CO_2 upwelling is not known), of which four studies reported no significant effect on growth rate of intermediate CO_2 levels (Langer et al., 2009; Shi et al., 2009; Richier et al.,

30   2011; Rokitta and Rost, 2012) compared to one which reported a decrease at 750 µatm (Iglesias-Rodriguez et al., 2008). For other *E. huxleyi* strains, results at intermediate CO_2 levels are not consistent among studies or between strains in the same study, while all strains tested at higher levels ($\leq$ 950 µatm) have shown slight to pronounced decreases in growth rate (Langer et al., 2009). Experiments were conducted at 15° C, with light intensities of 75 µmol photons m^{-2} s^{-1} in a 14:10 hour light:dark cycle. Culture media were prepared from seawater collected in wintertime from the Quintay coast (central Chile),

35   aged for >1 month, enriched with 176 µM nitrate, 7.2 µM phosphate, and with trace metals and vitamins as described for K/2 medium (Keller et al., 1987), and sterilized by filtration through 0.2 µm Stericups (Merck-Millipore, Billerica, MA, USA). Strains were acclimated to light and temperature conditions for at least two consecutive culture transfers, maintaining cell density below 200.000 cells ml^{-1} and ensuring exponential growth during the acclimation phase. Prior to inoculation, 4.5 L in 8 L cylindrical clear polycarbonate bottles (Nalgene) were continuously purged with humidified air with a pCO_2 of 400

40   and 1200 µatm for 24-48 hours to allow the carbonate system to equilibrate (controlled with pH readings) as described in

detail in Torres et al. (2013). When pH values had stabilized, these experimental bottles were inoculated at an initial density of 800 cells ml^{-1} (day 0). Daily measures of pH at 25° C were made using the indicator dye m-cresol purple with measurements of absorption at 578 nm, 434 nm, and 730 nm with a 1 cm path length as described in SOP6B (Dickson et al., 2007) with a BioSpec 1600 spectrophotometer (Shimadzu Scientific Instruments, Kyoto, Japan). Calculation of full

5   carbonate parameters were made from pH and measures of total alkalinity (AT) (measured as described above) taken on day 0 and at the end of the experiment, following protocols as described above for natural seawater samples.

Daily cell counts were performed from day 2 on using a Neubauer haemocytometer (as cells were too dilute for this method on day 0). Growth rate was calculated as specific growth rates μ (day^{-1}) = ln(N$_f$/N$_0$)/Δt, where N$_0$ and N$_f$ are the initial and final cell concentrations and Δt is the time interval (days). The experimental cultures were harvested when cell

10 concentrations were between 50,000 cells ml^{-1} and 100,000 cells ml^{-1}. Samples for measurement of particulate organic carbon (POC) and particulate inorganic carbon (PIC) were taken by filtering four 250 ml samples on 47 mm GF/F filters (pre-combusted for overnight at 500° C) which were then dried and stored in aluminium envelopes prior to measurement of C content by the Laboratorio de Biogeoquimica y Isotopos Estables Aplicados at the Pontificia Universidad Católica. For each culture, total carbon was measured on two replicate filters while POC was measured on two replicate filters after

15 treatment with fuming HCl. PIC was calculated as the difference between the two measures. POC and PIC concentrations were normalized to cell number, and POC and PIC production rates were obtained by multiplying cell normalized POC and PIC quotas with specific growth rates. Samples were filtered and processed as described above for SEM analysis. For flow cytometry, 1.8 ml samples were fixed by adding 0.2 ml of 10% formaldehyde/0.5% glutaraldehyde, 100 mM borate pH 8.5 (which was stored frozen and thawed immediately before use).

20 **2.5.1 SEM and flow cytometric assessments analysis of coccoliths**

Morphological analysis was performed on three replicates of each strain with a scanning electron microscope (Quanta 250) and images were analysed by ImageJ. Attached coccoliths were measured following Rosas-Navarro et al. (2016). On average, a total of 606 (min. 418) coccoliths per treatment were analysed. Coccoliths were classified into complete, incomplete and malformed (Rosas-Navarro et al., 2016). In the R/overcalcified strains, fusion of radial elements and the

25 over-growth of inner tube elements of the distal shield complicated finer scale assessments of coccolith formation. Therefore, we were highly conservative in categorizing coccoliths, and grouped incomplete and malformed coccoliths for statistical analysis. Of all coccolithospheres imaged, only coccoliths were selected for measurement which were oriented upwards (towards the beam) so that coccolith length measurements were not affected by viewing angle. This meant that an average of 68 coccoliths were measured per strain per treatment. Measurements included coccolith length, the total area of

30 the central area (defined by the inner end of distal shield radial elements), and the portion of the central area which was not covered by the inner tube.

Flow cytometry was performed using a BD InFlux equipped with a 488 nm laser and small particle detector with polarization optics. The laser, optics, and stream were aligned using 3 µm Ultra Rainbow Fluorescent Particles (Spherotech, Lake Forest, IL, USA). Trigger was set on forward scatter light with the same polarization as the laser, with trigger level

35 adjusted for each strain to ensure that all detached coccoliths could be detected. Cells were distinguished by red fluorescence (at 692 nm; due to chlorophyll). Detached coccoliths and calcified cells were distinguished as previously described (Von Dassow et al., 2012). Parameters analyzed included the number of detached coccoliths, percentage of calcified cells, relative change in depolarization of forward scatter light by detached coccoliths, and relative changes in red fluorescence (due to chlorophyll) of cells. All samples for a given treatment and strain were run on the same day with the same settings.

40 **2.6 Statistical analysis**

To test for significant correlations of environmental parameters (including carbonate chemistry) on coccolithophore community composition or *E. huxleyi* morphotype composition in the natural samples, Redundancy Analysis (RDA) was performed (see Supplement). For most analyses, we selected only data from the surface when multiple depths were available (see Supplementary Section S1 for comparison of surface to deeper samples).

5   Data from experimental results were analysed in Prism 6 (GraphPad Software, Inc., La Jolla, CA, USA) by 2-way ANOVA followed by Sidak post-hoc pairwise analysis with correction for multiple comparison. Prior to testing, PIC/POC ratio was log2-transformed while percentages (e.g. % area, % calcified cells) were expressed as proportions and arcsine-square-root transformed to permit use of parametric testing. Significance was judged at the $p < 0.05$ level.

3 Results

10 **3.1 Changes in coccolithophore species and *E. huxleyi* morphotypes in natural communities versus oceanographic conditions**

Surface pH (< 10 m depth) at sampling sites ranged from 7.73 (in the El Quisco 2012 sampling), to 8.11 (in the JF sampling). In terms of carbonate chemistry, the surface waters of the ESP showed a general pattern of increasing CO_2 and decreasing pH as one moves from open ocean waters to the Chilean coastal upwelling zones, however, as expected, waters

15 were never corrosive for calcite (Fig. 3a). More generally, the NBP and JF, as well as TON and QUI surveys were conducted in a relatively low (average 411.2 ± 41.3 µatm; $N_{samples} = 27$) and high (average 696.6 ± 110 µatm; $N_{samples} = 14$) CO_2 levels, respectively.

Coccolithophore numerical abundances ranged from 1×10^3 cells L^{-1} to 76×10^3 cells L^{-1} (59 total samples) (Fig. 3b). A total of 40 coccolithophore species were found inhabiting the Eastern South Pacific during the sampling period (Table S2).

20 Shannon diversity index ranged from 1.5 down to 0, while Fisher's alpha index ranged from 4.0 down to 0, and both indices showed coccolithophore diversity was lowest in the most acidified natural waters (Fig. 3a-b).

Five species of the Noëlaerhabdaceae family were observed, including *E. huxleyi*, *Gephyrocapsa ericsonii*, *G. muellerae*, *G. oceanica*, *G. parvula*, the last of which was recently re-assigned from the genus *Reticulofenestra* to the genus *Gephyrocapsa* (Bendif et al., 2016). The Noëlaerhabdaceae family numerically dominated all coccolithophore communities observed,

25 representing between 72.2% and 100% (average 94.1% ± 6.9%) of all coccolithophores in all samples observed. The most abundant coccolithophore outside this family was *Calcidiscus leptoporus*, present at 36% of stations and ranging in relative abundance from 0.9% to 25.4% (average 5.6% ± 6.9%). Within the Noëlaerhabdaceae, *E. huxleyi* was found in every sample, and exhibited relative abundances ranging from 15.5% to 100% of total coccolithophores (Fig. 3c). While *E. huxleyi* represented up to 100% of the coccolithophore community in high-CO_2 waters on the coast, it was observed in lower relative

30 abundances of samples taken further off shore, strongly correlating with the calculated diversity indices. *Gephyrocapsa ericsonii* and *G. parvula* were essentially excluded from high-CO_2 waters.

R/overcalcified morphotypes dominated *E. huxleyi* populations in high-CO_2 waters near the coast, representing on average 57.2% ± 22.9% (range 11% to 90%) (Fig. 3d). In contrast, moderately calcified A morphotype coccospheres dominated *E. huxleyi* populations in all low-CO_2 waters further off shore. (Fig. 3d). The other overcalcified morphotype A_CC, a form

35 characteristic of the Subtropical Front in the Western Pacific (Cubillos et al., 2007), represented less than 20% of total coccolithophores, and did not follow a clear pattern. The lightly calcified morphotypes were usually rare except in some of the samples from near Tongoy/Lengua de Vaca Point upwelling (Fig. 3d), where they seemed to be associated with intermediate CO_2 levels.

3.2 Phenotypes of *E. huxleyi* clonal isolates compared to natural populations from the high CO_2 and low CO_2 waters

Throughout the field campaigns, a total of 260 Noëlaerhabdaceae isolates were obtained and analyzed morphologically (Table 1; note that strains from stations nearby in time and space have been grouped). There was a bias towards isolating the dominant type within both the Noëlaerhabdaceae and *E. huxleyi* species complex at each station, and only 2% of the maintained isolates were from the *Gephyrocapsa* genus, suggesting that these closely related species are not as readily

5   cultured as *E. huxleyi*. The lightly calcified morphotype also remained poorly represented in culture compared to the natural communities, and the A_CC type appeared moderately over-represented. However, among the R/overcalcified and moderately calcified A morphotypes, the dominant morphotype obtained in culture always reflected the dominant morphotype in the natural community. Three representative R/overcalcified morphotypes strains, showing different degrees of overlap of the central area, and two representative A morphotype strains from offshore waters were chosen for

10   experimental analysis (Fig. 4).

3.3 Responses of different *E. huxleyi* morphotypes to OA

OA significantly reduced the growth rate in all strains and there was no significant interaction between strain and OA effects on growth rate (Fig. 5a; see Table 3 for global 2-way ANOVA statistics). OA increased POC quota (POC cell^{-1}) in all strains. However, the interaction between strain and OA was significant (Fig. 5b; Table 3). The increase in POC quota was

15   not significant in moderately calcified strains CHC428 and CHC440, while the hyper-calcified strain CHC342 exhibited the highest POC quota and the highest increase under OA conditions. The effect of OA on the POC production rate varied among strains: OA increased POC production in most strains, except for the moderately calcified strain CHC428 (Fig. 5c; Table 3). However, the change in POC production was significant in posthoc pairwise comparisons only for CHC342, in which it increased by 116% ($p < 0.0001$). With the exception of strain CHC342, neither the POC quota nor POC production

20   correlated with morphotype (R/overcalcified vs. A).

PIC/POC ratios dropped under OA in all strains (Fig. 5d). It is notable that the smallest changes in PIC/POC occurred in the two strains of moderately calcified morphotypes originating from offshore, low pCO_2 waters, not the strains with hyper- or heavily calcified morphotypes originating from coastal waters exposed to OA. However, although the effect of OA condition was globally significant across all strains (Table 3), in pairwise posthoc comparisons the drop in PIC/POC ratio was only

25   significant in CHC360 ($p = 0.005$). Also, the effect of strain on PIC/POC was not significant and there was no significant interaction between strain and OA (Table 3). PIC quotas varied among strains and the effect of OA also differed among strains (Fig. 5e; Table 3). The highest PIC quota was recorded in the hyper calcified strain CHC342 and the lowest in the moderately calcified strain CHC440. OA increased PIC quota significantly in strain CHC342 (pairwise posthoc test, $p = 0.0039$), but did not change PIC quota or the change was not significant in other strains. PIC production varied among strains

30   (Fig. 5f; Table 3) but there were no significant effects of OA or interaction between strain and OA (Table 3).

R/overcalcified coccoliths were not more resistant to OA than A morphotype coccoliths. OA significantly affected at least one morphological parameter measured in all but the A morphotype strain CHC440 (Fig. 4, Fig. 6). The coccosphere diameters did not change significantly under OA in any of the strains (Fig. 6d; Table 4). Coccolith lengths showed inconsistent and mostly insignificant changes among strains. In the global two-way ANOVA comparison, there was an

35   interaction between OA and strain (Table 4), but the only significant change under OA detected by posthoc pairwise comparisons between treatments was a small decrease in CHC428 under high CO_2 (Fig. 6e; $p = 0.0334$). The percentage of the central area that was uncovered by inner tube elements increased under OA (Fig. 6f). The significant interaction between strain and OA condition (Table 4) indicated that the effect of OA on this parameter varied among strains. It was most pronounced in strains CHC342 and CHC352, where the inner tube elements were heavily over-grown under low pCO_2,

40   whereas the effect was modest in the moderately calcified strains CHC428 and CHC440 (and not significant in pairwise posthoc tests of the effect of OA treatment within these strains; $p > 0.05$), where the central area was mostly exposed under both conditions. The incidence of incomplete or malformed coccoliths remained very low in all strains and treatments, but

OA caused a modest but significant increase (Fig. 6g; Table 4), ranging from between 0 and 1.3% of coccoliths under low CO_2 to between 1.4 and 6.6% under OA. This effect was greatest in R/overcalcified morphotype strains CHC342, CHC352, and CHC360, but there was no significant interaction between strain and OA treatment in the two-way ANOVA when all strains were considered (Table 4).

5 Flow cytometric analysis (see example cytograms in Fig. 7) showed significant changes in several cytometric parameters in response to OA, which in some cases varied among strains (Fig. 8; Table 5). Relative chlorophyll fluorescence was increased significantly in strains CHC360, CHC440, and CHC428, but dropped significantly in CHC352 (Fig. 8a, Table 5). The proportion of cells which were calcified was high (>97%) in all strains under the 400 µatm CO_2 control treatment but dropped modestly (0.04 to 7.2%) in all strains in the OA treatment (Fig. 8b). A significant interaction was detected between

10 strain and OA treatment in the proportion of cells calcified (Table 5), and this drop in response to OA was greatest in strains CHC360 (average change -7.2%) and CHC440 (average change -5.4%), which were the only two strains for which the difference between treatments was judged significant in pairwise post-hoc testing. In the control CO_2 treatment, the relative abundance of detached coccoliths, relative to the number of cells, was low (11.9 cell^{-1} to 14.4 cell^{1}) in most strains but high (63 ± 34 cell^{-1}) in strain CHC440. Despite significant variability among strains in the relative abundance of detached

15 coccoliths, there were no significant changes under OA (Fig. 8c; Table 5). The relative forward scatter depolarization (a proxy for the amount of calcite on a cell, see (Von Dassow et al., 2012) was decreased significantly under OA (Fig. 8d; Table 5), an effect which varied among strains (Table 5) and was strongest in strain CHC352. The relative scatter depolarization of detached coccoliths was also decreased under OA (Fig. 8e; Table 5), an effect that varied among strains, and was largest in CHC352 and CHC428.

20 **4 Discussion**

While an increasing number of studies have focused on examining the potential for adaptation to ocean acidification through long-term laboratory experiments, this study has taken an alternative approach, to test for local adaptation to short-term OA in populations of cosmopolitan phytoplankton found in waters that experience naturally acidified conditions due to upwelling of high CO_2 water. A similar approach has recently been taken in a variety of invertebrate species (Padilla-

25 Gamiño et al., 2016; Gaitán-Espitia et al., 2017; Vargas et al., 2017), finding both benthic/mero-planktonic animals, coralline algae, and holoplanktonic copepods do exhibit local adaptation in regions experiencing naturally high fluctuations in pH and CO_2.

This study confirms the presence of exceptionally robust over-calcified forms of *E. huxleyi* in the coastal zone of central to northern Chile. This was previously hinted from two sampling points/times, and now has been documented in separate years

30 (Beaufort et al., 2011). Overall, the presence of these morphotypes correlates with high CO_2 water. The use of targeted flow cytometry and cell sorting was successful in obtaining representatives of the different forms of *E. huxleyi* in mono-culture to test whether the correlation between phenotype and environment indeed reflected local adaptation. Two of the R/overcalcified strains chosen for experimental tests (CHC352 and CHC360) originated from the high CO_2 upwelling near Tongoy/Lengua de Vaca Point (Table 1). Strain CHC342 originated from Puñihuil along the outer (western) coast of Chiloe

35 Island (41.9° S). Although we lack carbonate system data from this site, the Chiloe Island is located approximately where the West Wind Drift arrives at the continent and turns north to form the Humboldt Current System (Thiel et al., 2007), so we considered CHC342, exhibiting a highly overcalcified R morphotype, might represent the southern end of the *E. huxleyi* populations which drift north and experience high CO_2/low pH upwelling conditions. We compared these three R/overcalcified strains to two A morphotype strains isolated from low CO_2 waters at a site 1000 km from the nearest shore.

40 Organisms in such waters are expected to experience very low fluctuations in pH (Hofmann et al., 2011), and so these strains were expected to exhibit low resistance to transient high CO_2/low pH conditions.

The bloom-former *E. huxleyi* is often considered a fast-growing, pioneer phytoplankton species (Paasche, 2002). However, calcification is costly and is most evidence suggests it may serve protective or defensive functions (Monteiro et al., 2016). Thus we considered both growth rate and calcification/morphological responses when analyzing potential adaptation. Surprisingly, we found no evidence that the exceptionally robust form was more resistant to high CO_2 than moderately calcified forms that seemed to be excluded from the high CO_2 upwelling waters.

The OA treatment reduced growth rate in all strains. The decrease in growth rate was accompanied by an increase in POC quota. This might suggest that cells were getting bigger, compensating for a decreased rate of cell division (as the increase in POC production rate was not significant in 4 of the 5 strains tested). However, the decrease in growth rate was also reflected in a decrease in culture *in vivo* fluorescence (data not shown), changes in coccosphere diameter were insignificant, and changes in cellular fluorescence measured by flow cytometry were small and consistent with only a small possible increase in cell biomass (and not in all strains, as CHC352 showed a decrease in this parameter). Among the few previous studies where a period of pre-acclimation to CO_2 was not used prior to growth measurements, inconsistent and non-significant effects of growth have been seen in two R morphotype strains NZEH (PLY M219) (Shi et al., 2009) and RCC1216 (Richier et al., 2011). Another study comparing several morphotypes isolated from the Southern Ocean reported that two "A/overcalcified" strains (similar to the R morphotype, but with distal shield radial elements not consistently fused) were resistant to similar OA treatments used here, while growth of both A and the lighter B/C morphotypes were strongly inhibited (Müller et al., 2015). Thus the strains R/overcalcified strains tested here, originating from high CO_2 environments, were surprisingly not resistant to high CO_2 in terms of growth rates.

In strain CHC342, POC quota increased to over 3x those previously reported in the literature for the species in response to high CO_2/low pH. This occurred in all four replicates, sampled at the same time as the low CO_2 replicates, so we have no evidence for this increase being a technical artefact. A similar increase in POC quota in response to high CO_2 has been reported in *Calcidiscus quadriperforatus* strain RCC 1168 to correlate with the production of transparent exopolysaccharides (TEP) (Diner et al., 2015), and so we suspect that the increase in POC/cell – at least in CHC342 – corresponds to increased TEP production.

As expected, PIC quotas varied among strains. CHC342, the strain showing the greatest degree of over-calcification, showed the highest PIC quota. Strain CHC440, the strain showing the coccoliths with the least percentage covering of the central area by the inner tube and the most delicate distal shield rim elements, showed the lowest PIC quota. However, the PIC quotas of CHC352, CHC360, and CHC428 were not different. The numbers of detached coccoliths per cell were similar among those three strains, but coccoliths produced by CHC428 were slightly larger, partly explaining this result. The PIC/POC ratio – considered important in determining the effect of coccolithophores on carbon export – also did not show consistent differences among morphotypes.

PIC/POC ratios decreased in all strains and all treatments, similar to most studies/strains which find that this parameter is negatively affected by acidification. However, in future studies it will be important to understand how TEP production impacts POC and PIC/POC ratios and responds to acidification, as has been shown in *Calcidiscus* (Diner et al., 2015). The effect of OA pH on calcification (PIC quota and PIC production) was variable among strains, with no clear pattern related to origin or calcification, and none of these modest effects were significant except the increase in PIC quote in CHC342, the most heavily calcified strain. While calcification rate appears to be sensitive to acidification in most studies/strains of *E. huxleyi* (Meyer and Riebesell, 2015) despite periods of acclimation, or even adaptation over hundreds of generations (Lohbeck et al., 2012), all of the strains tested here appear to be more similar in this aspect to strains found to exhibit calcification that is relatively resistant to OA (Langer et al., 2009). We did not see the dramatic loss of calcification (almost all cells were calcified in all strains and treatments) that was reported, for example, in a B/C morphotype from the Southern Ocean in response to OA (Müller et al., 2015).

A consensus of both microscopic and flow cytometric analysis measures indicated that coccolith morphology was not more resistant to high CO_2/low pH conditions in the R/overcalcified strains isolated from natural OA conditions in high CO_2 upwellings than in the A morphotype strains isolated from far offshore waters in equilibrium with the atmosphere, that are not known to experience natural OA episodes. The increase in the percentage of malformed or incomplete coccoliths in

5   response to high CO_2/low pH was most pronounced in the R/overcalcified morphotypes, although these percentaes remained low in all strains and both treatments compared to other studies. In other *E. huxleyi* morphotypes, the thickness of the tube around the coccolith central area is reported to decrease modestly under acidification conditions (Bach et al., 2012; Young et al., 2014), and a similar affect was seen in the two A morphotype strains here. In our study, this effect was most pronounced, resulting in a highly eroded appearance, in the most heavily over-calcified R strains, where the tube overgrows the central

10   area. Coccoliths are formed in intracellular compartments, and the extracellular $\Omega_{calcite}$ remained >1 in the experiments, so this must be due to effects on the formation of coccoliths, not erosion after coccolith secretion. This also shows that the degree of covering of the central area in these types depends on condition in the R morphotype, however, the principal morphotype classification of each of the 5 strains did not change, as expected if morphotype is genetically determined (Young and Westbroek, 1991). The disappearance of the underlying central area ("hollow coccoliths") reported in one study

15   (Lefebvre et al., 2012) was not observed here, but that effect was only reported in very high cell concentrations grown with high NH_4^+. The morphological observations by SEM were supported by flow cytometric results, which also showed changes in the relative depolarization of forward scatter light both of whole coccospheres and detached coccoliths.

The observation that the morphology and quality of coccoliths of moderately calcified A morphotype strains were comparatively little affected, while R/overcalcified forms were strongly affected, does not appear consistent with the

20   hypothesis that over-calcification of distal shield elements in the *E. huxleyi* present in naturally acidified high CO_2 water serves to compensate for OA effects on coccoliths. Some other factor must select for the R/overcalcified morphotype in the coastal zone of Chile. An A morphotype ("A*") exhibiting partial and irregular extension of inner tube elements over the central area (but not closure of spaces between distal shield radial elements) was dominant in the Benguela upwelling zone (not the more extreme R/overcalcified types) (Henderiks et al., 2012), while the A_CC type, although rare in front of Chile,

25   was dominant in the Northeast Atlantic (Bay of Biscay) in winter (Smith et al., 2012). The function of coccoliths is still not certain, but they may have a role in physical defense against grazing or bacterial attack (Jaya et al., 2016; Monteiro et al., 2016). It is interesting to speculate that high productivity conditions in eastern boundary coasts promote persistent higher abundances of grazers or phytopathogenic bacteria, against which the overcalcified coccoliths might provide better defense.

The lack of evidence for local adaptation (either in terms of growth or morphology) to short-term high CO_2/low pH

30   conditions in *E. huxleyi* populations that are naturally exposed to pulses of OA conditions, contrasts with the recent findings showing adaptation to ocean acidification in estuarine habitats in invertebrates and coralline algae (Padilla-Gamiño et al., 2016; Gaitán-Espitia et al., 2017; Vargas et al., 2017), including the neritic but holoplanktonic copepod *Acartia tonsa* (Vargas et al., 2017). Perhaps the Eastern South Pacific *E. huxleyi* populations – despite being relatively resistant – might already be near the limit to the ability of this organism to adapt to OA, suggesting this ubiquitous coccolithophore may not

35   be able to adapt to future ocean acidification in a way that preserves ecological and biogeochemical function. The consistent declines in both growth rates and PIC/POC ratios, even in genotypes that naturally are exposed to OA conditions, supports the prediction that PIC-associated POC export may decline, potentially weakening the biological pump (Hofmann and Schellnhuber, 2009).

Author contributions

40   PD led the study, carried out sampling in field surveys, performed flow cytometric isolation of *E. huxleyi* strains, carried out statistical analysis of experimental data, supervised processing of samples by flow cytometry and electron microscopy, and

wrote the manuscript. FDR conducted characterization of coccolithophore communities and *E. huxleyi* morphotype composition, analysed the relationships of coccolithophore communities and *E. huxleyi* morphotypes to environmental parameters, assisted with part of the OA experiments in the Calfuco Marine Laboratory, and helped prepare the first draft of the manuscript and figures. EMB participated in field studies in 2012, helped with classification of *E. huxleyi* morphotypes,

5 and trained and supervised FDR. in coccolithophore taxonomic classification. JDGE led experimental work in the Calfuco laboratory and provided key comments and editing of the manuscript. SR provided insights into interpretation of results and edited a draft of the manuscript. DM helped plan and perform experiments in the Calfuco lab. UJ assisted with initial plans and later interpretations. RT performed chemical analysis on seawater samples and helped set up the Calfuco Marine Laboratory experiments.

10

The authors declare they have no conflicts of interest.

References

25 Armstrong, R. A., Lee, C., Hedges, J. I., Honjo, S. and Wakeham, S. G.: A new, mechanistic model for organic carbon fluxes in the ocean based on the quantitative association of POC with ballast minerals, Deep. Res. Part II Top. Stud. Oceanogr., 49(1–3), 219–236, doi:10.1016/S0967-0645(01)00101-1, 2002.

Bach, L. T., Bauke, C., Meier, K. J. S., Riebesell, U. and Schulz, K. G.: Influence of changing carbonate chemistry on morphology and weight of coccoliths formed by Emiliania huxleyi, Biogeosciences, 9(8), 3449–3463, doi:10.5194/bg-9-
30 3449-2012, 2012.

Baith, K., Lindsay, R., Fu, G. and McClain, C. R.: SeaDAS, a data analysis system for ocean-color satellite sensors., Eos, Trans. Am. Geophys. Union, 82(18), 202–202, doi:10.1029/01EO00109, 2001.

Beaufort, L., Probert, I., de Garidel-Thoron, T., Bendif, E. M., Ruiz-Pino, D., Metzl, N., Goyet, C., Buchet, N., Coupel, P., Grelaud, M., Rost, B., Rickaby, R. E. M. and de Vargas, C.: Sensitivity of coccolithophores to carbonate chemistry and
35 ocean acidification, Nature, 476(7358), 80–83, doi:10.1038/nature10295, 2011.

Bendif, E. M., Probert, I., Díaz-Rosas, F., Thomas, D., van den Engh, G., Young, J. R. and von Dassow, P.: Recent reticulate evolution in the ecologically dominant lineage of coccolithophores, Front. Microbiol., 7, 784, doi:10.3389/fmicb.2016.00784, 2016.

Brady Olson, M., Wuori, T. A., Love, B. A. and Strom, S. L.: Ocean acidification effects on haploid and diploid Emiliania
40 huxleyi strains: Why changes in cell size matter, J. Exp. Mar. Bio. Ecol., 488, 72–82, doi:10.1016/j.jembe.2016.12.008, 2017.

Cubillos, J. C., Wright, S. W., Nash, G., Salas, M. F. De, Griffiths, B., Tilbrook, B., Poisson, A. and Hallegraeff, G. M.: Calcification morphotypes of the coccolithophorid Emiliania huxleyi in the Southern Ocean: changes in 2001 to 2006

compared to historical data, Mar. Ecol. Prog. Ser., 348, 47–54, doi:10.3354/meps07058, 2007.

Von Dassow, P., Van Den Engh, G., Iglesias-Rodriguez, D. and Gittins, J. R.: Calcification state of coccolithophores can be assessed by light scatter depolarization measurements with flow cytometry, J. Plankton Res., 34(12), 1011–1027, doi:https://doi.org/10.1093/plankt/fbs061, 2012.

5   Dickson, A. G. and Millero, F. J.: A comparison of the equilibrium constants for the dissociation of carbonic acid in seawater media, Deep. Res. Part A. Oceanogr. Res. Pap., 34(10), 1733–1743, doi:10.1016/0198-0149(87)90021-5, 1987.

Dickson, A. G., Sabine, C. L. and Christian, J. R., Eds.: Guide to Best Practices for Ocean CO2 Measurements., PICES Special Publication 3, Victoria, BC, Canada., 2007.

Diner, R. E., Benner, I., Passow, U., Komada, T., Carpenter, E. J. and Stillman, J. H.: Negative effects of ocean acidification

10   on calcification vary within the coccolithophore genus Calcidiscus, Mar. Biol., 162(6), 1287–1305, doi:10.1007/s00227-015-2669-x, 2015.

Engel, A., Zondervan, I., Aerts, K., Beaufort, L., Benthien, A., Chou, L., Delille, B., Gattuso, J.-P., Harlay, J., Heemann, C., Hoffmann, L., Jacquet, S., Nejstgaard, J., Pizay, M.-D., Rochelle-newall, E., Schneider, U., Terbrueggen, A. and Riebesell, U.: Testing the direct effect of CO2 concentration on a bloom of the coccolithophorid Emiliania huxleyi in mesocosm

15   experiments, Limnol. Oceanogr., 50(2), 493–507, 2005.

Frankignoulle, M., Canon, C. and Gattuso, J.: Marine calcification as a source of carbon dioxide: Positive feedback of increasing atmospheric CO2, Limnol. Oceanogr., 39(2), 458–462, 1994.

Friederich, G. E., Ledesma, J., Ulloa, O. and Chavez, F. P.: Air-sea carbon dioxide fluxes in the coastal southeastern tropical Pacific, Prog. Oceanogr., 79(2–4), 156–166, doi:10.1016/j.pocean.2008.10.001, 2008.

20   Gaitán-Espitia, J. D., Villanueva, P. A., Lopez, J., Torres, R., Navarro, J. M. and Bacigalupe, L. D.: Spatio-temporal environmental variation mediates geographical differences in phenotypic responses to ocean acidification, Biol. Lett., 13, 20160865, doi:http://dx.doi.org/10.1098/rsbl.2016.0865, 2017.

Hagino, K., Bendif, E. M., Young, J. R., Kogame, K., Probert, I., Takano, Y., Horiguchi, T., de Vargas, C. and Okada, H.: New evidence for morphological and genetic variation in the cosmopolitan coccolithophore Emiliania huxleyi

25   (Prymnesiophyceae) from the cox1b-atp4 genes, J. Phycol., 47(5), 1164–1176, doi:10.1111/j.1529-8817.2011.01053.x, 2011.

Henderiks, J., Winter, A., Elbrächter, M., Feistel, R., Van Der Plas, A., Nausch, G. and Barlow, R.: Environmental controls on Emiliania huxleyi morphotypes in the Benguela coastal upwelling system (SE Atlantic), Mar. Ecol. Prog. Ser., 448, 51–66, doi:10.3354/meps09535, 2012.

30   Heraldsson, C., Anderson, L. G., Hassellöv, M., Hulth, S. and Olsson, K.: Rapid, high-precision potentiometric titration of alkalinity in ocean and sediment pore waters, Deep. Res. Part I Oceanogr. Res. Pap., 44(12), 2031–2044, doi:10.1016/S0967-0637(97)00088-5, 1997.

Hofmann, G. E., Smith, J. E., Johnson, K. S., Send, U., Levin, L. A., Micheli, F., Paytan, A., Price, N. N., Peterson, B., Takeshita, Y., Matson, P. G., de Crook, E., Kroeker, K. J., Gambi, M. C., Rivest, E. B., Frieder, C. A., Yu, P. C. and Martz,

35   T. R.: High-frequency dynamics of ocean pH: A multi-ecosystem comparison, PLoS One, 6(12), e28983, doi:10.1371/journal.pone.0028983, 2011.

Hofmann, M. and Schellnhuber, H.-J.: Oceanic acidification affects marine carbon pump and triggers extended marine oxygen holes, Proc. Natl. Acad. Sci., 106(9), 3017–3022, doi:10.1073/pnas.0813384106, 2009.

Iglesias-Rodriguez, M. D., Halloran, P. R., Rickaby, R. E. M., Hall, I. R., Colmenero-Hidalgo, E., Gittins, J. R., Green, D. R.

40   H., Tyrrell, T., Gibbs, S. J., von Dassow, P., Rehm, E., Armbrust, E. V. and Boessenkool, K. P.: Phytoplankton calcification in a high-CO2 world, Science (80-.)., 320(5874), 336–340, doi:10.1126/science.1154122, 2008.

Iglesias-Rodríguez, M. D., Brown, C. W., Doney, S. C., Kleypas, J., Kolber, D., Kolber, Z., Hayes, P. K. and Falkowski, P. G.: Representing key phytoplankton functional groups in ocean carbon cycle models: Coccolithophorids, Global

Biogeochem. Cycles, 16(4), 47-1-47–20, doi:10.1029/2001GB001454, 2002.

Jaya, B. N., Hoffmann, R., Kirchlechner, C., Dehm, G., Scheu, C. and Langer, G.: Coccospheres confer mechanical protection: New evidence for an old hypothesis, Acta Biomater., 42, 258–264, doi:10.1016/j.actbio.2016.07.036, 2016.

Jin, P., Ding, J., Xing, T., Riebesell, U. and Gao, K.: High levels of solar radiation offset impacts of ocean acidification on
5 calcifying and non-calcifying strains of Emiliania huxleyi, Mar. Ecol. Prog. Ser., 568, 47–58, 2017.

Keller, M. D., Selvin, R. C., Claus, W. and Guillard, R. R.: Media for the culture of oceanic ultraphytoplankton, J. Phycol., 23(4), 633–638, 1987.

Krueger-Hadfield, S. A., Balestreri, C., Schroeder, J., Highfield, A., Helaouët, P., Allum, J., Moate, R., Lohbeck, K. T., Miller, P. I., Riebesell, U., Reusch, T. B. H., Rickaby, R. E. M., Young, J. R., Hallegraeff, G., Brownlee, C. and Schroeder,
10 D. C.: Genotyping an Emiliania huxleyi (Prymnesiophyceae) bloom event in the North Sea reveals evidence of asexual reproduction, Biogeosciences, 11, 5215–5234, doi:10.5194/bg-11-5215-2014, 2014.

Langer, G., Nehrke, G., Probert, I., Ly, J. and Ziveri, P.: Strain-specific responses of Emiliania huxleyi to changing seawater carbonate chemistry, Biogeosciences Discuss., 6(2), 4361–4383, doi:10.5194/bgd-6-4361-2009, 2009.

Lefebvre, S. C., Benner, I., Stillman, J. H., Parker, A. E., Drake, M. K., Rossignol, P. E., Okimura, K. M., Komada, T. and
15 Carpenter, E. J.: Nitrogen source and pCO$_2$ synergistically affect carbon allocation, growth and morphology of the coccolithophore Emiliania huxleyi: Potential implications of ocean acidification for the carbon cycle, Glob. Chang. Biol., 18(2), 493–503, doi:10.1111/j.1365-2486.2011.02575.x, 2012.

Litchman, E., de Tezanos Pinto, P., Edwards, K. F., Klausmeier, C. A., Kremer, C. T. and Thomas, M. K.: Global biogeochemical impacts of phytoplankton: A trait-based perspective, J. Ecol., 103(6), 1384–1396, doi:10.1111/1365-
20 2745.12438, 2015.

Lohbeck, K. T., Riebesell, U. and Reusch, T. B. H.: Adaptive evolution of a key phytoplankton species to ocean acidification, Nat. Geosci., 5(12), 917–917, doi:10.1038/ngeo1637, 2012.

McDonald, M. J., Rice, D. P. and Desai, M. M.: Sex speeds adaptation by altering the dynamics of molecular evolution, Nature, 531(7593), 233–236, doi:10.1038/nature17143, 2016.

25 Mehrbach, C., Culberson, C. H., Hawley, J. E. and Pytkowicz, R. M.: Measurment of the apparent dissociation constants of carbonic acid in seawater at atmospheric pressure, Limnol. Oceanogr., 18(6), 897–907, 1973.

Meyer, J. and Riebesell, U.: Reviews and syntheses: Responses of coccolithophores to ocean acidification: A meta-analysis, Biogeosciences, 12(6), 1671–1682, doi:10.5194/bg-12-1671-2015, 2015.

Monteiro, F. M., Bach, L. T., Brownlee, C., Bown, P., Rickaby, R. E. M., Poulton, A. J., Tyrrell, T., Beaufort, L.,
30 Dutkiewicz, S., Gibbs, S., Gutowska, M. A., Lee, R., Riebesell, U., Young, J. and Ridgwell, A.: Why marine phytoplankton calcify, Sci. Adv., 2(7), e1501822–e1501822, doi:10.1126/sciadv.1501822, 2016.

Müller, M. N., Trull, T. W. and Hallegraeff, G. M.: Differing responses of three Southern Ocean Emiliania huxleyi ecotypes to changing seawater carbonate chemistry, Mar. Ecol. Prog. Ser., 531, 81–90, 2015.

Müller, M. N., Trull, T. W. and Hallegraeff, G. M.: Independence of nutrient limitation and carbon dioxide impacts on the
35 Southern Ocean coccolithophore Emiliania huxleyi, ISME J., Advance On, 1–11, doi:10.1038/ismej.2017.53, 2017.

Orr, J. C., Fabry, V. J., Aumont, O., Bopp, L., Doney, S. C., Feely, R. A., Gnanadesikan, A., Gruber, N., Ishida, A., Joos, F., Key, R. M., Lindsay, K., Maier-Reimer, E., Matear, R., Monfray, P., Mouchet, A., Najjar, R. G., Plattner, G.-K., Rodgers, K. B., Sabine, C. L., Sarmiento, J. L., Schlitzer, R., Slater, R. D., Totterdell, I. J., Weirig, M.-F., Yamanaka, Y. and Yool, A.: Anthropogenic ocean acidification over the twenty-first century and its impact on calcifying organisms, Nature, 437(7059),
40 681–686, doi:10.1038/nature04095, 2005.

Paasche, E.: A review of the coccolithophorid Emiliania huxleyi (Prymnesiophyceae) with particular reference to growth, coccolith formation, and calcification-photosynthesis interactions, Phycologia, 40(6), 503–529, doi:http://dx.doi.org/10.2216/i0031-8884-40-6-503.1, 2002.

Padilla-Gamiño, J. L., Gaitán-Espitia, J. D., Kelly, M. W. and Hofmann, G. E.: Physiological plasticity and local adaptation to elevated pCO2 in calcareous algae : an ontogenetic and geographic approach, Evol. Appl., 9(2016), 1043–1053, doi:10.1111/eva.12411, 2016.

Pierrot, D., Lewis, D. E. and Wallace, D. W. R.: CO2SYS. EXE—MS excel program developed for CO2 system 5 calculations., [online] Available from: http://cdiac.ornl.gov/ftp/co2sys, 2006.

Poulton, A. J., Young, J. R., Bates, N. R. and Balch, W. M.: Biometry of detached Emiliania huxleyi coccoliths along the Patagonian Shelf, Mar. Ecol. Prog. Ser., 443, 1–17, doi:10.3354/meps09445, 2011.

Richier, S., Fiorini, S., Kerros, M. E., von Dassow, P. and Gattuso, J. P.: Response of the calcifying coccolithophore Emiliania huxleyi to low pH/high pCO2: From physiology to molecular level, Mar. Biol., 158(3), 551–560, 2011.

10 Riebesell, U., Zondervan, I., Rost, B., Tortell, P. D., Zeebe, R. E. and Morel, F. M.: Reduced calcification of marine plankton in response to increased atmospheric CO2., Nature, 407(6802), 364–7, doi:10.1038/35030078, 2000.

Riebesell, U., Bach, L. T., Bellerby, R. G. J., Monsalve, J. R. B., Boxhammer, T., Czerny, J., Larsen, A., Ludwig, A. and Schulz, K. G.: Competitive fitness of a predominant pelagic calcifier impaired by ocean acidification, Nat. Geosci., 10(1), 19–23, doi:10.1038/NGEO2854, 2017.

15 Rokitta, S. D. and Rost, B.: Effects of CO2 and their modulation by light in the life-cycle stages of the coccolithophore Emiliania huxleyi, Limnol. Oceanogr., 57(2), 607–618, doi:10.4319/lo.2012.57.2.0607, 2012.

Rosas-Navarro, A., Langer, G. and Ziveri, P.: Temperature affects the morphology and calcification of Emiliania huxleyi strains, Biogeosciences, 13(10), 2913–2926, doi:10.5194/bg-13-2913-2016, 2016.

Sabine, C. L., Feely, R. A., Gruber, N., Key, R. M., Lee, K., Bullister, J. L., Wanninkhof, R., Wong., C. S., Wallace, D. W. 20 R., Tilbrook, B., Millero, F. J., Peng, T.-H., Kozyr, A., Ono, T. and Rios, A. F.: The Oceanic Sink for Anthropogenic CO2, Science (80-.)., 305(5682), 367–371, doi:10.1126/science.1097403, 2004.

Sanders, R., Morris, P. J., Poulton, A. J., Stinchcombe, M. C., Charalampopoulou, A., Lucas, M. I. and Thomalla, S. J.: Does a ballast effect occur in the surface ocean?, Geophys. Res. Lett., 37(8), 1–5, doi:10.1029/2010GL042574, 2010.

Schlüter, L., Lohbeck, K. T., Gröger, J. P., Riebesell, U. and Reusch, T. B. H.: Long-term dynamics of adaptive evolution in 25 a globally important phytoplankton species to ocean acidification, Sci. Adv., 2(7), e1501660–e1501660, doi:10.1126/sciadv.1501660, 2016.

Shi, D., Xu, Y. and Morel, F. M. M.: Effects of the pH / pCO 2 control method on medium chemistry and phytoplankton growth, Biogeosciences, 6(7), 1199–1207, doi:10.5194/bg-6-1199-2009, 2009.

Smith, H. E. K., Tyrrell, T., Charalampopoulou, A., Dumousseaud, C., Legge, O. J., Birchenough, S., Pettit, L. R., Garley, 30 R., Hartman, S. E., Hartman, M. C., Sagoo, N., Daniels, C. J., Achterberg, E. P. and Hydes, D. J.: Predominance of heavily calcified coccolithophores at low CaCO3 saturation during winter in the Bay of Biscay, Proc. Natl. Acad. Sci., 109(23), 8845–8849, doi:10.1073/pnas.1117508109, 2012.

Smith, S. V.: Parsing the oceanic calcium carbonate cycle: a net atmospheric carbon dioxide source, or a sink?, L&O e-Books. Association for the Sciences of Limnology and Oceanography Inc, Waco, TX USA., 2013.

35 Thiel, M., Macaya, E. C., Acuña, E., Arntz, W. E., Bastias, H., Brokordt, K., Camus, P. A., Castilla, J. C., Castro, L. R., Cortés, M., Dumont, C. P., Escribano, R., Fernández, M., Gajardo, J. A., Gaymer, C. F., Gomez, I., González, A. E., González, H. E., Haye, P. A., Illanes, J. E., Iriarte, J. L., Lancelloti, D. A., Luna-Jorquera, G., Luxoro, C., Manriquez, P. H., Marín, V., Muñoz, P., Navarretes, S. A., Perez, E., Poulin, E., Sellanes, J., Sepúlveda, H. H., Stotz, W., Tala, F., Thomas, A., Vargas, C. A., Vasquez, J. A. and VegaA, J. M. A.: The Humboldt current system of northern and central Chile 40 Oceanographic processes, ecological interactions and socioeconomic feedback, Oceanogr. Mar. Biol., 45, 195–344, doi:10.1201/9781420050943, 2007.

Torres, R., Pantoja, S., Harada, N., González, H. E., Daneri, G., Frangopulos, M., Rutllant, J. A., Duarte, C. M., Rúiz-Halpern, S., Mayol, E. and Fukasawa, M.: Air-sea CO2 fluxes along the coast of Chile: From CO2 outgassing in central

northern upwelling waters to CO2 uptake in southern Patagonian fjords, J. Geophys. Res. Ocean., 116(9), 1–17, doi:10.1029/2010JC006344, 2011.

Torres, R., Manriquez, P. H., Duarte, C., Navarro, J. M., Lagos, N. A., Vargas, C. A. and Lardies, M. A.: Evaluation of a semi-automatic system for long-term seawater carbonate chemistry manipulation, Rev. Chil. Hist. Nat., 86(4), 443–451,

5   doi:10.4067/S0716-078X2013000400006, 2013.

Vargas, C. A., Lagos, N. A., Lardies, M. A., Duarte, C., Manríquez, P. H., Aguilera, V. M., Broitman, B., Widdicombe, S. and Dupont, S.: Species-specific responses to ocean acidification should account for local adaptation and adaptive plasticity, Nat. Ecol. Evol., 1(4), 84, doi:10.1038/s41559-017-0084, 2017.

Young, J. R. and Westbroek, P.: Genotypic variation in the coccolithophorid species Emiliania huxleyi, Mar.

10   Micropaleontol., 18, 5–23, doi:10.1016/0377-8398(91)90004-P, 1991.

Young, J. R., Geisen, M., Cros, L., Kleijne, A., Sprengel, C., Probert, I. and Østergaard, J. B.: A guide to extant coccolithophore taxonomy, J. Nannoplankt. Res., Special Is, 1–125, 2003.

Young, J. R., Poulton, A. J. and Tyrrell, T.: Morphology of Emiliania huxleyi coccoliths on the northwestern European shelf - Is there an influence of carbonate chemistry?, Biogeosciences, 11(17), 4771–4782, doi:10.5194/bg-11-4771-2014, 2014.

15

Biogeosciences
Discussions

Open Access

EGU

Table 1. Noëlaerhabdaceae strains isolated during this study. All sites near Tongoy were grouped in 2011 and in 2012, as were the sites at JF in 2011.

Site	Total strains	*E. huxleyi*				Other species		
		R/over	A_CC	A	Light	*G muel.*	*G eric.*	*G parv.*
TON 2011	132	85%	10%	2%	1%	2%	0%	0%
JF 2011	34	32%	35%	32%	0%	0%	0%	0%
TON 2012[a]	20	90%	10%	0%	0%	0%	0%	0%
Puñi. 2012[b]	10	40%	20%	40%	0%	0%	0%	0%
NBP H1	15	0%	33%	67%	0%	0%	0%	0%
NBP H10[c]	28	0%	21%	55%[c]	24%	0%	0%	0%
NBP BB2	21	0%	33%	43%	0%	0%	5%	19%

[a] Site represented by strains CHC352 and CHC360

[b] Site represented by strain CHC342

5 [c] Site represented by strains CHC428 and CHC440

Table 2. Carbonate system parameters during experiment. Means of experimental replicates at the time of inoculation (T_{inoc} and harvesting (T_{final}) are given. The last two rows give the average and maximum standard deviations between replicates among all strains. pCO_2 units are µatm, alkalinity units are µmol kg^{-1}.

Strain	Treat	pCO_2		Alkalinity		pH		$\Omega_{calcite}$	
		T_{inoc}	T_{final}	T_{inoc}	T_{final}	T_{inoc}	T_{final}	T_{inoc}	T_{final}
342	400	422	332	2260	1839	8.020	8.029	3.53	2.89
	1200	1314	1257	2264	2207	7.574	7.582	1.40	1.40
352	400	402	370	2292	2168	8.042	8.052	3.59	3.49
	1200	1226	1341	2274	2168	7.601	7.565	1.44	1.34
360	400	441	457	2270	2126	8.005	7.965	3.55	3.08
	1200	1186	1409	2289	2254	7.623	7.545	1.65	1.37
428	400	440	419	2261	2157	8.004	8.004	3.54	3.33
	1200	1259	1247	2262	2250	7.592	7.592	1.52	1.49
440	400	457	382	2254	2114	7.988	8.033	3.26	3.47
	1200	1486	1249	2261	2235	7.522	7.591	1.24	1.51
Ave. std dev.	400	22	18	8	17	0.018	0.016	0.12	0.13
	1200	38	69	7	11	0.012	0.020	0.04	0.06
Max. std dev.	400	38	48	13	25	0.033	0.040	0.23	0.27
	1200	95	156	12	20	0.033	0.043	0.11	0.13

5

Table 3. Global 2-way ANOVA results for growth and biogeochemical parameters of strains exposed to high CO_2/low pH conditions versus control CO_2 treatment. PIC/POC values were log2-transformed prior to testing.

		Growth rate	POC	POC prod	PIC	PIC prod	PIC/POC
Source of variat.	Interact.	2.63 %	21.7 %	18.8 %	10.3 %	6.00 %	8.15 %
	Strain	13.7 %	62.8 %	77.5 %	71.3 %	69.2 %	10.9 %
	CO_2	60.9 %	23.0 %	9.67 %	3.68 %	2.13 %	37.8 %
F-values	Interact.	$F_{4,29} = 0.926$	$F_{4,25} = 36.1$	$F_{4,25} = 27.0$	$F_{4,25} = 3.08$	$F_{4,25} = 1.65$	$F_{4,25} = 1.15$
	Strain	$F_{4,29} = 4.83$	$F_{4,25} = 105$	$F_{4,25} = 111.0$	$F_{4,25} = 21.3$	$F_{4,25} = 19.0$	$F_{4,25} = 1.54$
	CO_2	$F_{1,29} = 85.7$	$F_{1,25} = 153$	$F_{1,25} = 55.6$	$F_{1,25} = 4.38$	$F_{1,25} = 2.33$	$F_{1,25} = 21.3$
p-values	Interact.	0.463	< 0.0001	< 0.0001	0.0343	0.194	0.358
	Strain	0.0041	< 0.0001	< 0.0001	< 0.0001	< 0.0001	0.222
	CO_2	< 0.0001	< 0.0001	< 0.0001	0.0466	0.139	0.0001

Table 4. Global 2-way ANOVA results for coccosphere and coccolith parameters of strains exposed to high CO_2/low

5 **pH conditions versus control CO_2 treatment. Proportions of central area covered and of incomplete or malformed coccoliths were arcsine-squareroot-transformed prior to testing.**

		Coccosphere diameter	Coccolith length	Proportion central area covered	Proportion of coccoliths incompl. or malform.
Source of variat.	Interact.	7.58 %	34.7 %	12.3 %	4.40 %
	Strain	53.7 %	25.3 %	53.3 %	18.0 %
	CO_2	4.76 %	0.396 %	29.2 %	55.4 %
F-values	Interact.	$F_{4,19} = 1.071$	$F_{4,19} = 4.62$	$F_{4,19} = 21.9$	$F_{4,19} = 1.18$
	Strain	$F_{4,19} = 7.595$	$F_{4,19} = 3.37$	$F_{4,19} = 94.7$	$F_{4,19} = 4.83$
	CO_2	$F_{1,19} = 2.689$	$F_{1,19} = 0.211$	$F_{1,19} = 207$	$F_{1,19} = 59.6$
p-values	Interact.	0.398	0.0090	< 0.0001	0.351
	Strain	0.0008	0.0304	< 0.0001	0.0074
	CO_2	0.118	0.652	< 0.0001	< 0.0001

19

Table 5: Global 2-way ANOVA results for flow cytometric parameters. The percentages of calcified cells were expressed as a fraction and arcsine-squareroot-transformed prior to testing.

		Rel. red fluoresce.	% calcified	# detached coccol.	Rel. scatter depol. cells	Rel. scatter depol. detached liths
Source of variat.	Interact.	35.0 %	18.9 %	2.27 %	11.2 %	7.85 %
	Strain	34.7 %	6.42 %	67.8 %	55.8 %	57.9 %
	CO_2	13.5 %	38.7 %	1.09 %	25.4 %	22.8 %
F-values	Interact.	$F_{3,20} = 16.0$	$F_{3,20} = 3.62$	$F_{3,20} = 0.525$	$F_{3,20} = 36.5$	$F_{3,20} = 12.3$
	Strain	$F_{3,20} = 15.9$	$F_{3,20} = 1.23$	$F_{3,20} = 15.7$	$F_{3,20} = 182$	$F_{3,20} = 90.6$
	CO_2	$F_{1,20} = 18.5$	$F_{1,20} = 22.2$	$F_{1,20} = 0.757$	$F_{1,20} = 249$	$F_{1,20} = 107$
p-values	Interact.	< 0.0001	0.0309	0.670	< 0.0001	< 0.0001
	Strain	< 0.0001	0.326	< 0.0001	< 0.0001	< 0.0001
	CO_2	0.0003	0.0001	0.395	< 0.0001	< 0.0001

5
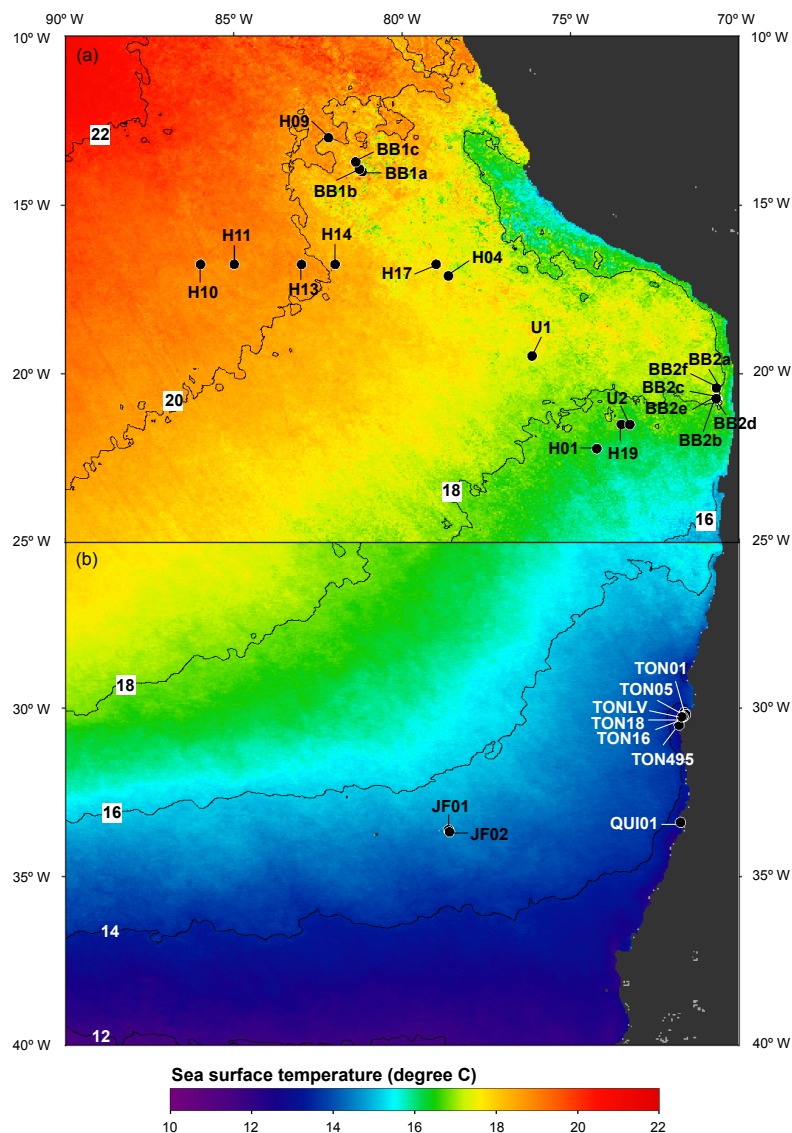
Figure 1: Map of stations sampled during NBP 1305 cruise (Jun.-Jul. 2013) (a) and in smaller field expeditions of Oct.-Nov. in 2011-2012 (b). SST climatologies (2002-2012) are plotted for the month of July (a) and October (b).
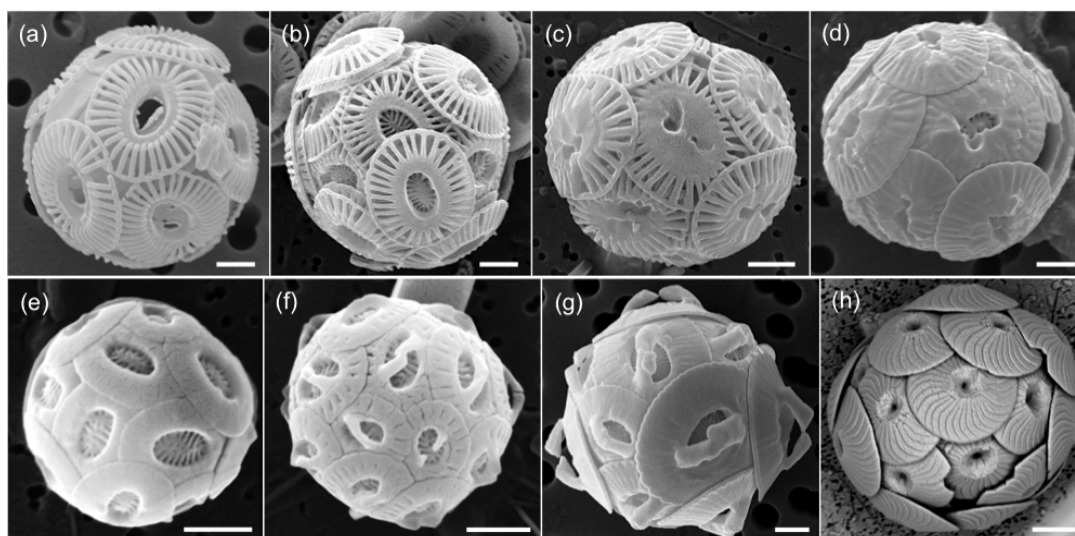
Figure 2: The most abundante coccolithophores in the SE Pacific. (a-d) Morphotypes of *E. huxleyi*: Lightly calcified (a), moderately calcified A morphotype (b), morphotype A_CC (c), morphotype R/overcalcified (d). *Gephyrocapsa* 5 ***parvula* (e), *G. ericsonii* (f), *G. muellerae* (g), and *Calcidiscus leptoporus*. Scale bars are 1 µm (a-g) and 3 µm in (h).**
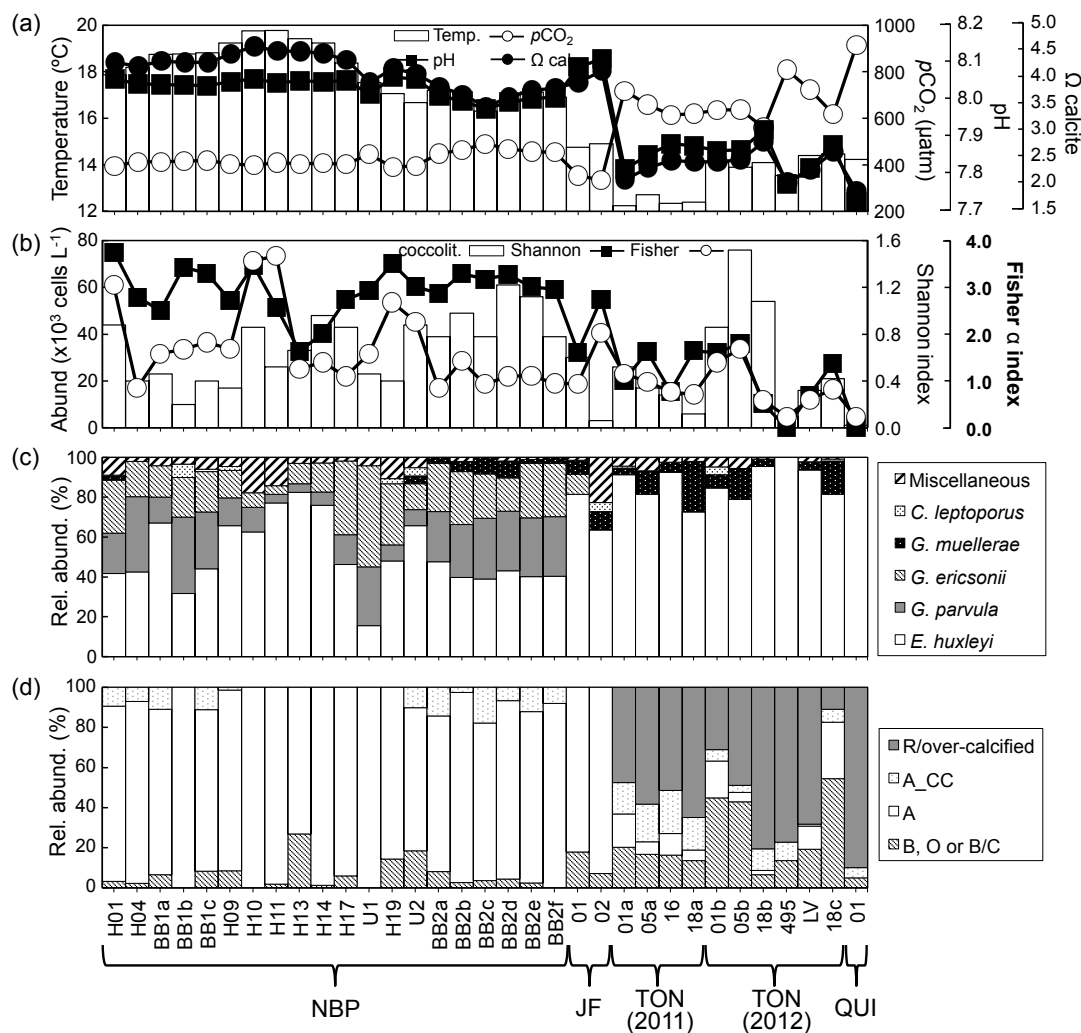
Figure 3: Environmental conditions, coccolithophore community, and *E. huxleyi* morphotypes. (a) Temperature, pH, CO_2, and $\Omega_{calcite}$. (b) Coccolithophore abundance, and Shannon and Fisher's alpha diversity indices. (c) Relative abundance of principal coccolithophore taxa. (d) Relative abundance of *E. huxleyi* morphotypes. The lightly calcified morphotypes B, O, and B/C have been grouped together.
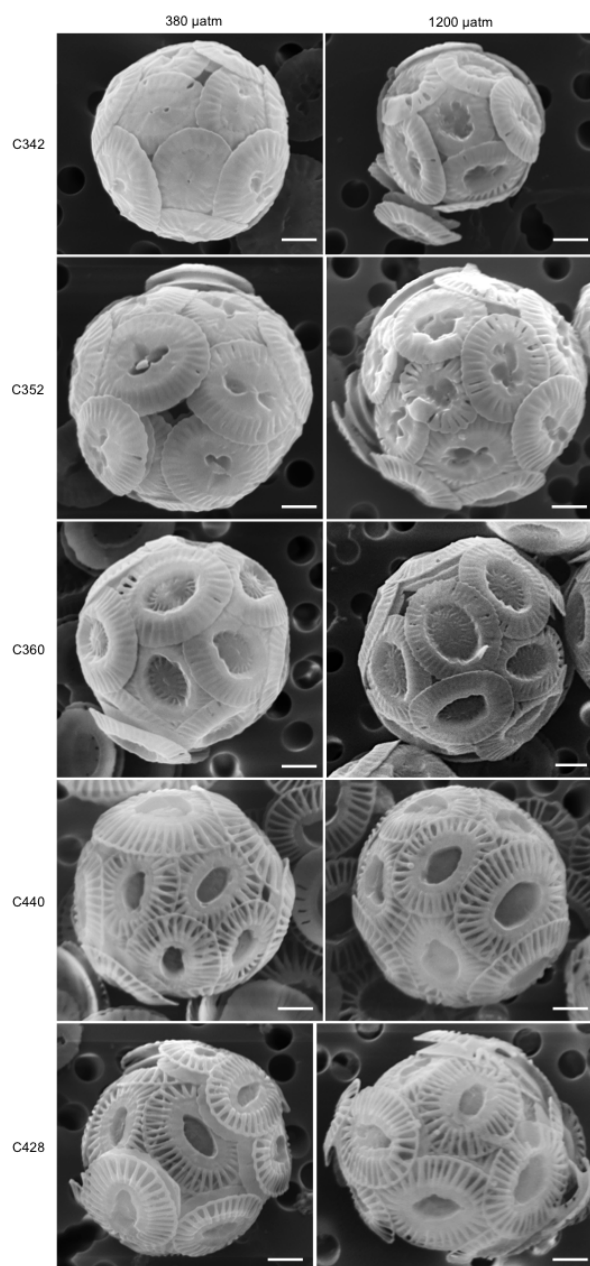
Figure 4: Representative coccospheres from each strain and treatment tested in the experiment. CHC342 was isolated from the Pacific coast of Chiloe (41.9° S, 74.0° W) in Nov. 2012, CHC352 and CHC360 were isolated from the Punta Lengua de Vaca upwelling center (30.3° S, 71.7° W) in Nov. 2012. CHC440 and CHC428 were isolated from the farthest west station in the Pacific (station H10, at 16.7° S, 86° W) during the NBP1305 cruise in Jul. 2013.
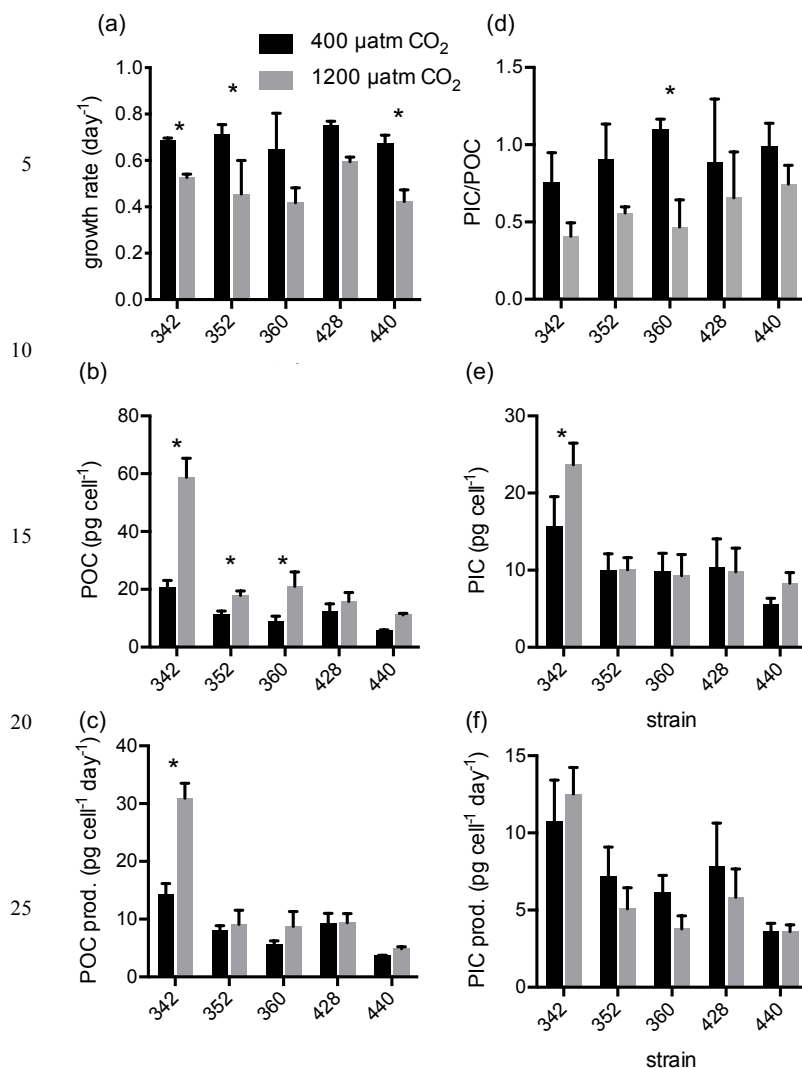
Figure 5: Growth rates (a), POC quotas (b), POC production rates (c), PIC/POC (d), PIC quotas (e), and PIC production rates (f) of *E. huxleyi* strains in response to 400 µatm (black bars) and 1200 µatm (grey bars) CO$_2$ treatments. See Table 3 for global two-way ANOVA results. * indicates significant difference ($p < 0.05$) in pairwise comparison between the two CO$_2$ treatments for a given strain, as judged by Sidak posthoc testing with correction for multiple comparison.
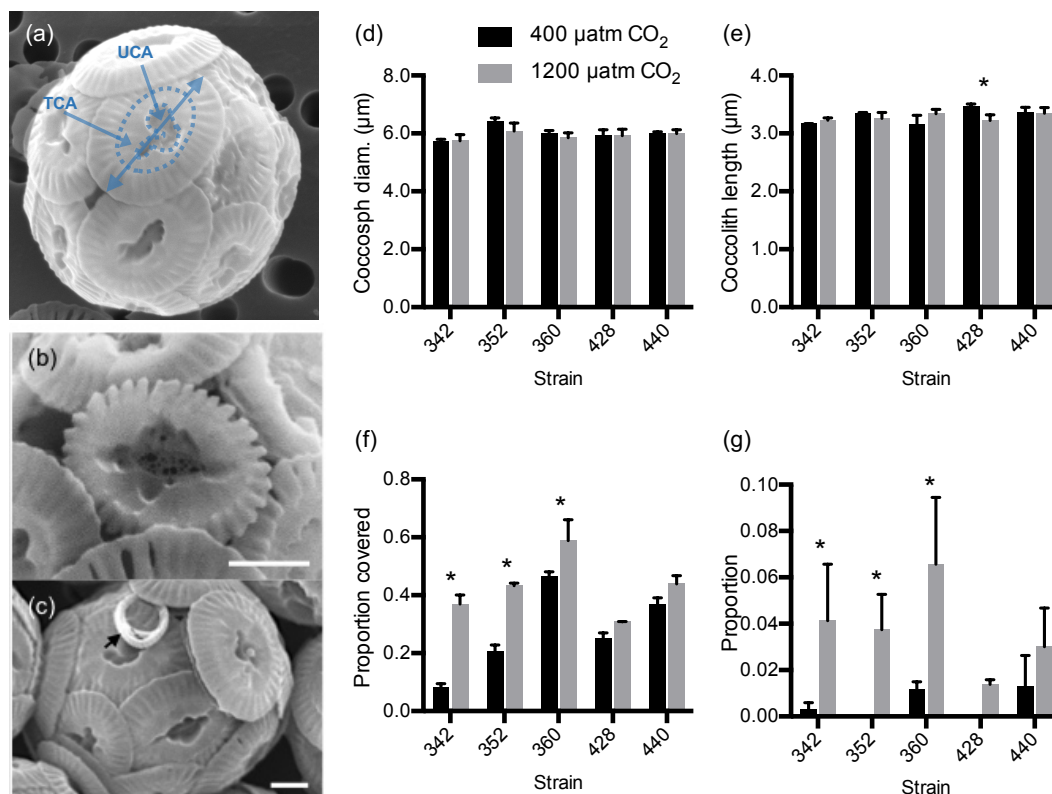
Figure 6: Effects of high CO_2/low pH conditions on coccolithophore morphology. (a) Example illustrating coccolith measurements taken including coccolith length (solid line with two arrow heads), total central area/inner tube (TCA) (defined by inner terminal of radial elements), and the part of the central area that is uncovered by tube elements (UCA). (b) Example of a coccolith classified as incomplete/malformed. (c) Example of a very incomplete coccolith (arrow). (d) Coccosphere diameters. (e) Coccolith length. (f) Proportion of central area not covered. (g) Proportion of coccoliths that were malformed or incomplete. See Table 4 for global two-way ANOVA results. * indicates significant difference ($p < 0.05$) in pairwise comparison between the two CO_2 treatments for a given strain, as judged by Sidak posthoc testing with correction for multiple comparison.

(a)

(b)

5
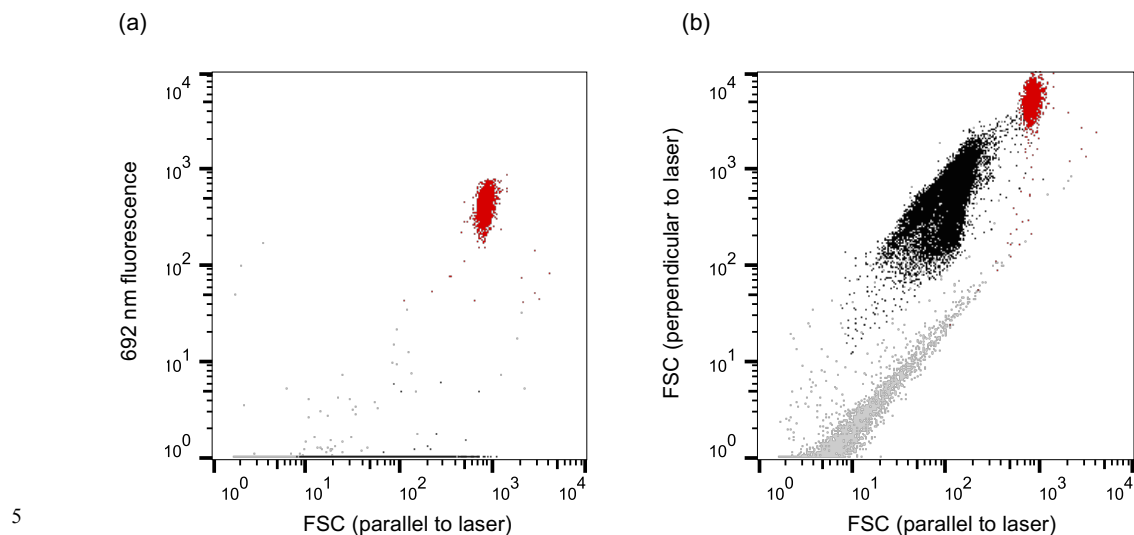
Figure 7: Example flow cytograms (of CHC352 at 400 µatm CO$_2$) showing identification of chlorophyll-containing (red fluorescent cells) in plot of 692 nm (40 nm band pass) fluorescence (y-axis) vs forward scatter with polarization
10 **parallel to laser (FSC) (a) and cytogram of scatter depolarization (FSC with polarization perpendicular to laser vs FSC with polarization parallel to laser) (b). Chlorophyll-containing cells are represented by red dots, black dots represent detached coccoliths, and grey dots represent other particles, which are mostly not optically active and fall on a straight line in panel b.**
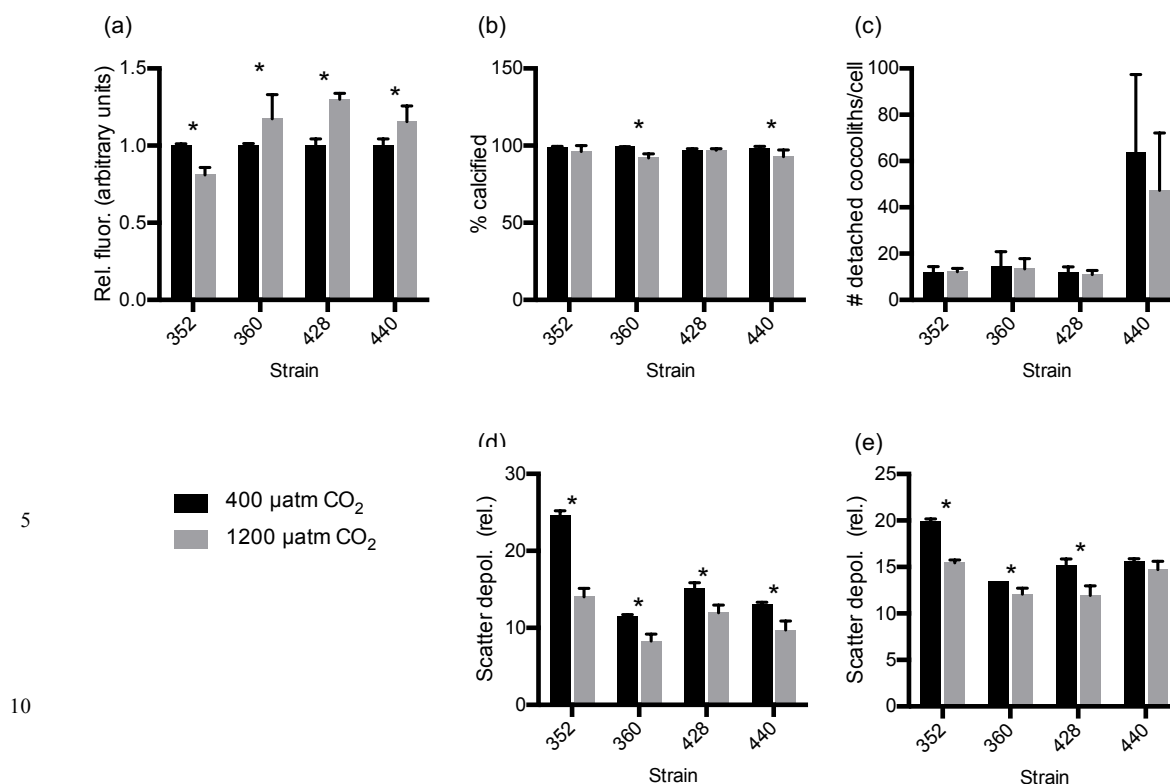
15

Figure 8. Effects of high CO_2 treatment on flow cytometric properties of cells and detached coccoliths for all treatments and strain. Strain CHC342 is not shown because samples were lost in transit between labs. Shown are the relative fluorescence (compared to control treatment) (a), the proportion of cells that were calcified (b), abundance of detached coccoliths divided by cell abundance (c), relative FSC (scatter depolarization) of cells (d) and detached coccoliths (e). Fluorescence and FSC units are relative and the voltage for the detector for FSC perpendicularly polarized was two-fold higher, resulting in approximately two orders of magnitude higher sensitivity. Scatter depolarization was calculated for every particle as the ratio of FSC with polarizations perpendicular vs parallel to the laser, normalized by the same ratio for non-optically active particles within the same sample. * indicates significant difference ($p < 0.05$) in pairwise comparison between the two CO_2 treatments for a given strain, as judged by Sidak posthoc testing with correction for multiple comparison.